Reduction of Low Space Harmonics for the Fractional Slot Concentrated Windings Using a Novel Stator Design

Gurakuq Dajaku[1], Wei Xie[2], and Dieter Gerling[2]

[1]FEAAM GmbH, Neubiberg D-85577, Germany
[2]Universitaet der Bundeswehr Muenchen, Neubiberg D-85577, Germany

Using magnetic flux barriers in the stator yoke of electric machines with fractional slots, tooth-concentrated winding, it is possible to reduce or even to cancel some space harmonics of low order in the air-gap flux density resulting in lower rotor losses induced by the armature reaction field. In this paper, this new technique is applied during the design and analysis of two permanent magnet machines with different 12-teeth/10-poles concentrated windings. Considering the main machine performances, such as the electromagnetic torque, machine losses, and also the field-weakening capability, the new stator design shows significant advantages over the conventional design. According to the new technique, a prototype machine is built and some measurement results are given.

Index Terms— **Efficiency, finite-element method (FEM), loss reduction, magnetic flux barrier, magnetomotive force (MMF) harmonics, permanent magnet (PM) synchronous machines, tooth-concentrated winding.**

NOMENCLATURE

B	Flux density (T).
I	Stator current (A).
i_d	Phase current, d-axis, (A).
i_q	Phase current, q-axis, (A).
L_d	Machine inductance, d-axis, (H).
L_q	Machine inductance, q-axis, (H).
R_m	Flux path magnetic reluctance (m^2/H).
u	Voltage (V).
T_e	Electromagnetic torque (Nm).
ϕ_1	Magnetic flux (Vs).
ψ_d^m	PM flux linkage, d-axis, (Vs).
ψ_q^m	PM flux linkage, q-axis, (Vs).
n_1	Number of turns per coil side.
w	Number of turns per phase.
ν	MMF stator space harmonic.

I. INTRODUCTION

RECENTLY, permanent magnet (PM) synchronous machines with fractional slot concentrated windings (FSCWs) have been widely used in several industry applications. The use of concentrated windings offers the advantage of short and less complex end winding, high slot filling factor, low cogging torque, greater fault tolerance, and low manufacturing costs. The stator coils may be wound either on all the teeth (double-layer winding) or only on alternate teeth (single-layer winding) and the manufacturing of these windings may be much cheaper because they contain simple coils that can be wounded automatically. Furthermore, using FSCW, different combinations of numbers of poles and numbers of slots are possible [1]–[4]. However, the magnetic field of these windings has more space harmonics, including subharmonics. For the PM machines, the torque is developed by the interaction of a specific high stator space harmonic with the permanent magnets. On other side, the rest of the sub and high harmonics, which rotate with the different speed and also in opposite directions, lead to undesirable effects, such as additional stator and rotor iron losses, eddy-current loss in the magnets [5]–[9], and noise and vibrations [10]–[13], which are the main disadvantages of these winding types.

To improve the magnetomotive force (MMF) winding performances of the FSCW regarding to power losses and noise problems, several methods and techniques have been developed and investigated in the past [14]–[22]. References [14]–[20] show different methods for the reduction of winding subharmonics, such as using multilayer tooth concentrated windings [14]–[17], winding coils with different turns per coil side [18], or magnetic flux barriers in the specific stator core locations [19], [20]. Furthermore, in [21] and [22], two another new solutions for reducing simultaneously the sub and high MMF harmonics of the FSCW by increasing the number of stator slots and using two winding systems are presented. The investigations carried out on these methods show enormous improvements on the PM machine performances, such as reduction of the sub and high MMF harmonics more than 60%, reduction of radial force modes of low order, reduction of the machine losses (magnet losses, iron losses, and so on), improved cooling capability (direct cooling of coil windings), reduction in the slot proximity effects, and so on.

In this paper, the new stator structure with magnetic flux barriers in stator yoke is investigated in detail by considering two different concentrated winding types. Using the new stator topology, two PM machines with the 12-teeth/10-poles single- and double-layer winding are considered and their performances are compared with the conventional stator. The main objective of this paper is to investigate the flux barrier effect on the electromagnetic torque, losses, machine parameters, and also on the field-weakening capability of the considered electric machines. The design and analysis of

Manuscript received June 28, 2013; revised October 8, 2013; accepted December 6, 2013. Date of publication December 11, 2013; date of current version May 1, 2014. Corresponding author: G. Dajaku (e-mail: gurakuq.dajaku@unibw.de).

Color versions of one or more of the figures in this paper are available online at http://ieeexplore.ieee.org.

Digital Object Identifier 10.1109/TMAG.2013.2294754

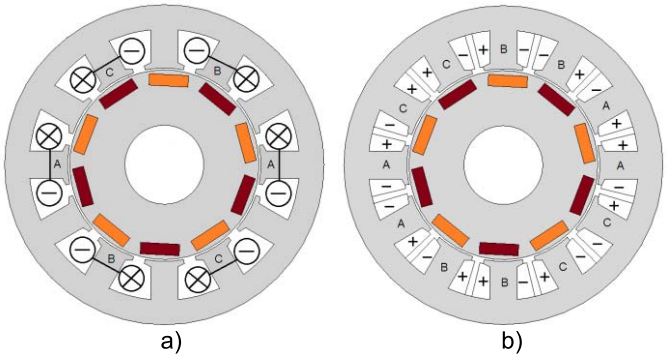

Fig. 1. Two 12-teeth/10-poles PM machines. (a) Single-layer winding. (b) Double-layer winding.

the studied machines is performed using 2-D finite-element method (FEM). For the PM machine with the double-layer winding, a prototype machine with the new stator structure is built and the first measurement results for the machine torque, machine efficiency, current quality, and also the no-load voltage are given.

II. 12-Teeth/10-Poles Concentrated Winding

As well as is mentioned previously, there are many possible slot number and pole number combinations for PM machines with concentrated windings. The winding layout and the winding factor of a PM machine with concentrated winding depend on its combination of pole and slot number. Therefore, this combination should be chosen carefully to maximize the fundamental (MMF working harmonic) winding factor and thus the torque density. Single-layer windings are preferred to double-layer windings when a high fundamental winding factor and high fault tolerance is required. Otherwise, double-layer windings are preferable to limit the losses and torque ripple.

Fig. 1 shows two PM machines with 12-teeth in the stator and 10-poles in the rotor and with different concentrated winding layouts. Single-layer winding have coils wound only on alternate teeth, whereas each tooth of the double-layer windings carries a coil. The corresponding MMF harmonics for these winding types are shown in Fig. 2. As well is shown, for both presented winding types, the first, fifth, seventh, 17th, and 19th are the dominant space harmonics and usually for different machine designs, the fifth or the seventh harmonic is mostly used as working harmonics. For the 10-pole machine, however, only the fifth stator space harmonic interacts with the field of the PMs to produce continuous torque. The other MMF space harmonics, in particular, the first, seventh, 17th, and so on, which have relatively large magnitudes, are undesirable and in some cases, they limit the usefulness of this winding type in different specific applications.

Let us be reminded here that the main difference between the presented winding types is not only in the winding layout, but, for the single-layer winding, the winding factors for the fifth, seventh, and so on are about 3.3% higher compared with the double-layer winding. However, as shown in Fig. 2, the amplitude of the first MMF subharmonic is relatively too

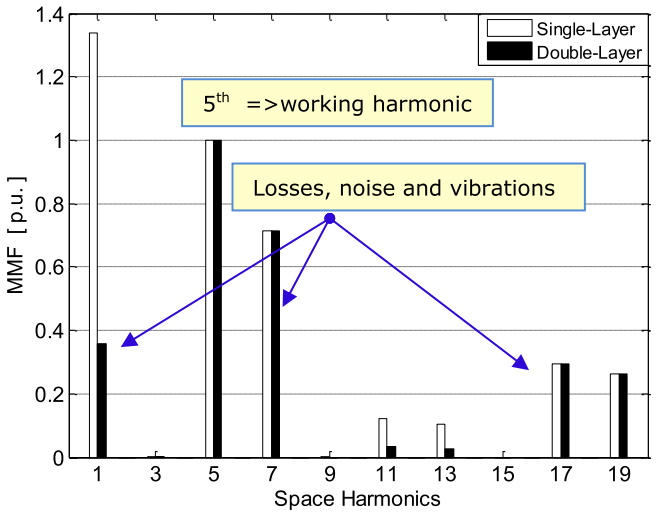

Fig. 2. MMF winding harmonics for the 12-teeth/10-poles single- and double-layer winding.

high, which induces huge losses in the rotor core and magnets, and thus it decreases the torque density and the efficiency of the machine. As results, the PM machines with the double-layer winding are mostly used in many applications.

III. Reduction of MMF Winding Subharmonics Using Magnetic Flux Barriers in Stator Yoke

A. Reduction of Subharmonics Using Coils With Different Turns Per Coil Side

A simple method for reducing the subharmonics for the tooth concentrated windings using winding coils with different number of turns per coil side is developed in [18]. Fig. 3(a) shows the basic idea for the reduction of subharmonics using concentrated coils with different turns per coil side, the winding layout is shown in Fig. 3(b); however, Fig. 3(c) shows the MMF distribution of one phase for the new 12-teeth/10-poles winding. For the sake of simplicity, only the winding coils of phase-A are presented in the sketch, with n_1 and n_2 denoting the number of turns per coil sides of one winding coil. In the new winding, the relation between n_1 and n_2 is

$$n_1 = n_2 - 1, \qquad \text{and} \quad 50\% \le n_1/n_2 < 100\%.$$

From [18], the analytical function for the MMF of the 12-teeth/10-poles new winding can be described using

$$\Theta(x,t) = \sum_{\nu} \frac{m}{2} \cdot \frac{2 \cdot w \cdot {}^{\nu}\xi_{w,\text{new}}}{\pi \nu} \cdot \hat{i} \cdot \cos\left(\omega t - \nu \frac{\pi}{\tau_p} x + \delta\right) \tag{1}$$

where the winding factor for the concentrated winding with different turns per coil side is

$${}^{\nu}\xi_{w,\text{new}} = \frac{2n_1}{n_2+n_1} \cos\left(\nu \frac{5}{12}\pi\right) \cdot \sin\left(\nu \frac{\pi}{12}\right) + \frac{n_1-n_2}{n_2+n_1} \sin\left(\nu \frac{\pi}{3}\right). \tag{2}$$

In (1), m is number of phases, ${}^{\nu}\xi_{w,\text{new}}$ is the winding factor, $\hat{i}$ is the phase current amplitude, δ is the current load angle,

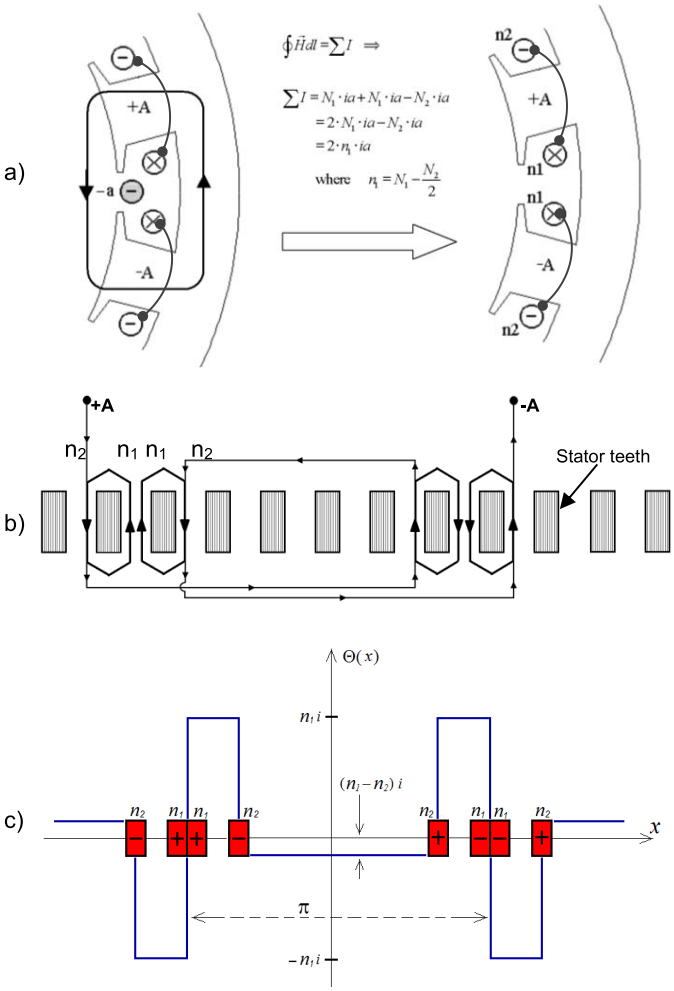

Fig. 3. (a) Realization of the new winding according to [18]. (b) Winding layout of phase-A. (c) MMF distribution (phase-A) for the new winding.

ω is the angular frequency, w is the number of turns per phase, and ν are MMF winding harmonics.

Investigations on the winding factors for the MMF harmonics according to (2) show that for the n_1/n_2 relation between 80% and 90%, e.g., $n_1/n_2 = 6/7, 7/8, 8/9$, and so on, the first subharmonic of the considered winding type can be reduced more than 90%; however, the working (fifth) harmonic remains quasi uneffected (less than 0.45%). It is important to point out that the presented technique is useful only for the double (multi) layer concentrated windings. However, an alternative solution for reducing the winding subharmonics for the single and also the multilayers tooth-concentrated windings is presented in [19].

B. New Stator Core With Magnetic Flux Barriers

Fig. 4 shows once again the new 12-teeth/10-poles machine (coil groups of one phase) using coils with different turns per coil side. Under one-phase excitation condition, the flux lines due to stator currents flow through the neighbor teeth around the slot, which contains the coil side of one phase. The magnetic flux can be determined in simple form using the well-known relation between the flux ϕ, magnetic

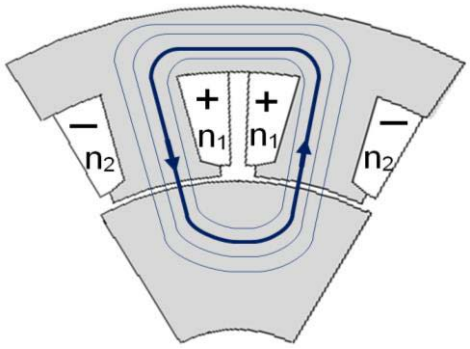

Fig. 4. Electric machine with the new 12-teeth/10-poles winding. Flux line distribution under one-phase load condition.

reluctance R_m, and the winding MMF Θ_S

$$\phi = \Theta_S / R_m. \tag{3}$$

For the machine section shown in Fig. 4, according to Ampere's law, the slot MMF (slot-1) is

$$\Theta_S = 2n_1 \cdot i. \tag{4}$$

However, R_m represents the total magnetic reluctance of flux path.

From (3) and (4), the resulting magnetic flux under one-phase load condition is

$$\phi = \frac{2n_1 \cdot i}{R_m}. \tag{5}$$

Then, according to the first method presented above and (5), the effect of winding subharmonics can be reduced by reducing the stator MMF in specific slots, or by increasing the magnetic reluctance in specific stator core location as described in the following.

Case I: New winding and conventional stator core

$$\begin{aligned} \Theta_{S,I} &= 2n_1 \cdot i \\ R_{m,I} &= 2R_0 + 2R_1 + R_2 + R_3 \\ \phi_I &= \frac{2n_1 \cdot i}{R_{m,I}}. \end{aligned} \tag{6}$$

Case II: Conventional winding and new stator core

$$\begin{aligned} \Theta_{S,II} &= 2n \cdot i, \quad n_1 = n_2 = n \\ R_{m,II} &= 2R_0 + 2R_1 + R_2^* + R_3 \\ \phi_{II} &= \frac{2n \cdot i}{R_{m,II}}. \end{aligned} \tag{7}$$

Fig. 5 shows a simple magnetic equivalent circuit (MEC) for the 12-teeth/10-poles electric machine with the new stator structure. With R_0–R_3 denoted the magnetic reluctances of corresponding magnetic flux paths. R_2 and R_2^* represent the magnetic reluctances of the stator yoke region for the conventional and also the new stator structure, respectively. Therefore, from (6), (7), and Fig. 5, the reduction of the subharmonic effect can be reached also with the convectional

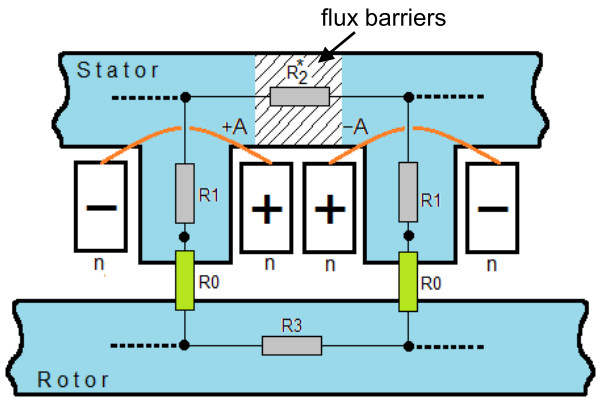

Fig. 5. MEC for the new stator structure.

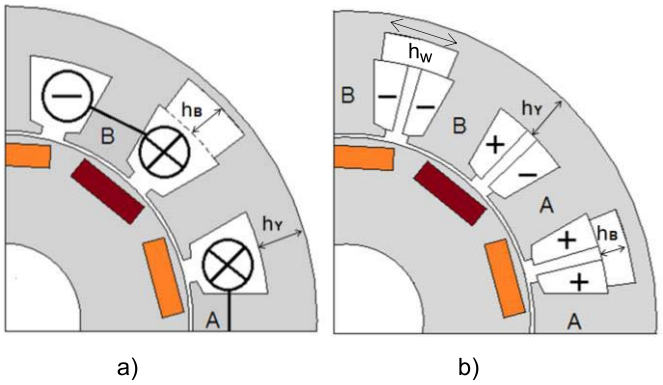

Fig. 6. New 12-teeth/10-poles PM machines with concentrated winding. (a) Single-layer winding. (b) Double-layer winding.

winding ($n_1 = n_2 = n$), however, by modifying (increasing) the magnetic reluctance R_2^{*1} in stator yoke.

From (6) and (7), the stator yoke reluctance for the new stator structure should be

$$\phi_I = \phi_{II} \Rightarrow R_2^* = k_w \cdot R_2 + (1 - k_w) \cdot R_e' \tag{8}$$

with

$$k_w = \frac{n_2}{n_2 - 1} \quad \text{and} \quad 1 < k_w \leq 2$$
$$R_e' = 2R_0 + 2R_1 + R_3.$$

C. Flux Barrier Effect on the Air-Gap Flux Density Subharmonics

To show the effect of the magnetic flux barriers on the air-gap flux density subharmonics, the both single- and double-layer 12-teeth/10-poles windings are considered in the following. Fig. 6(a) and (b) shows the geometries of the studied PM machines with the new stator core structure, with h_Y denoting the stator yoke thickness, h_w the flux barrier width, and h_B the flux barrier depth. As is described also in the previous section, for the double-layer winding, the flux barriers should be placed on the yoke region beside the stator slots, which includes the coil sides of the same phase; however, for the single-layer case, the flux barriers can be used beside any second slot.

[1]Each magnetic resistance can be modified to fulfill the required condition; however, the magnetic resistance of the stator yoke is the single resistance, which fulfills the above requirements without influencing the flux density of neighboring slots.

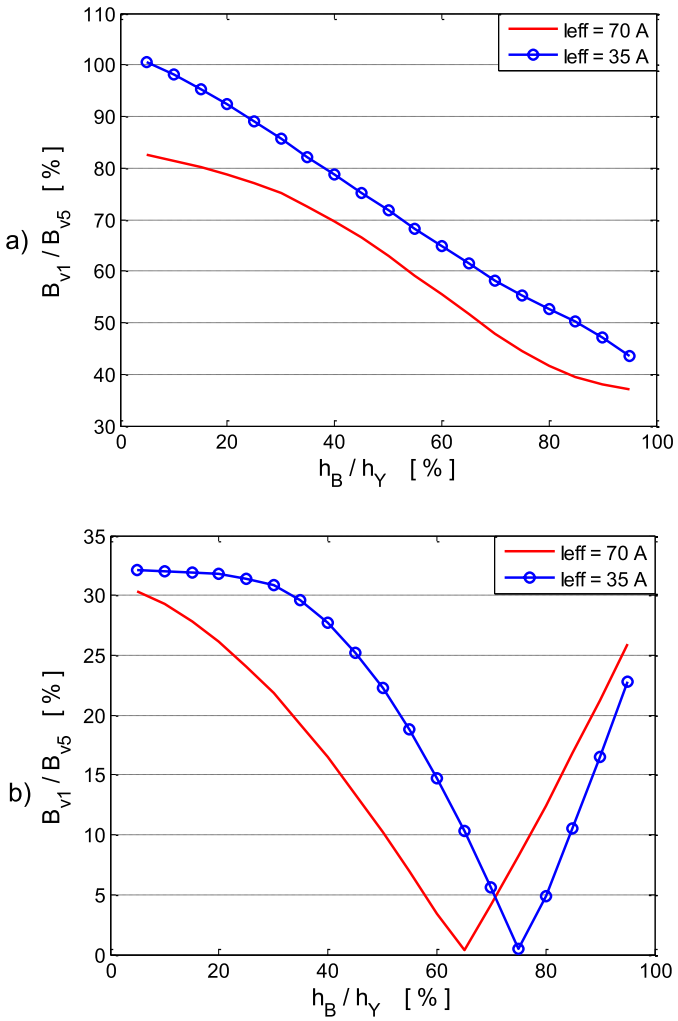

Fig. 7. Flux barrier effect on the first air-gap flux density harmonic. (a) Single-layer winding. (b) Double-layer winding.

For the given machine geometries, Fig. 7(a) and (b) shows the effect of the flux barriers depth on the air-gap flux density harmonics due to reaction fields. Using FEM, the simulations are performed for different load currents, and the resulting air-gap flux density harmonics are observed for $h_B = 0$ to 100% h_Y. Only the first subharmonic is considered and the obtained results are presented as a relative ratio to the fifth working harmonic, $B_{\nu=1}/B_{\nu=5}$. It can be observed here that, for the electric machine with the double-layer winding, the first subharmonic completely can be canceled by choosing a proper flux barrier width. Depending on the excitation load current, the h_B parameter varies between 65% to 80% of h_Y. On the other side, for the single-layer winding, a complete cutout of the yoke region reduces the first subharmonic to about 60%.

IV. Design and Analysis of Two 12-Teeth/10-Poles PM Machines for Automotive Application

Using the new stator structure, two PM machines with the new stator structure and 12-teeth/10-poles single- and

TABLE I
MAIN GEOMETRY DATA

Outer rotor diameter	*48 mm*
Outer stator diameter	*81 mm*
Gap length	*0.5 mm*
Magnet length (magn. direction)	*3 mm*
Magnet width	*10 mm*
Active length	*70 mm*
Turns per phase	*20*
Number of stator teeth	*12*
Number of rotor poles	*10*

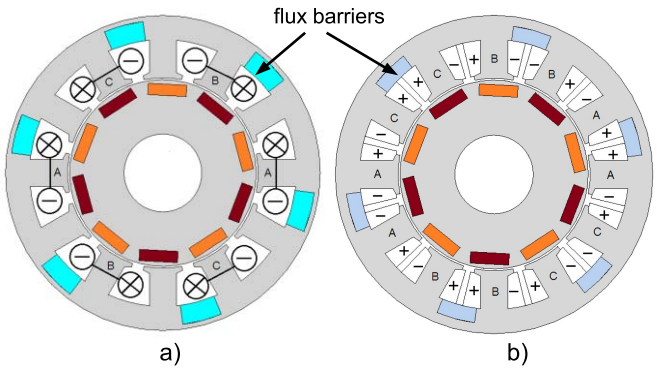

Fig. 8. Considered PM machines with the new stator core structure. (a) Single-layer winding. (b) Double-layer winding.

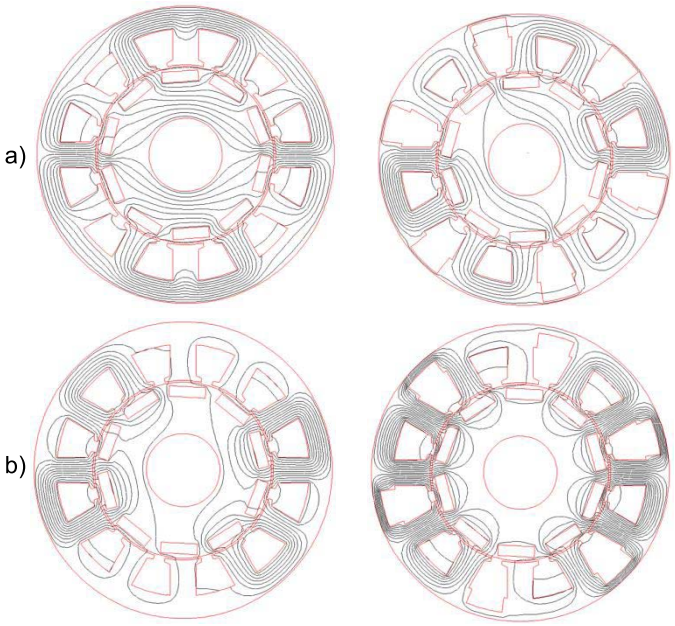

Fig. 9. Flux density distribution due to the armature reaction field. (a) Single-layer winding. (b) Double-layer winding.

double-layer concentrated winding are designed and analyzed, and their characteristics are compared with the conventional stator design. The geometries and the main geometry data of the studied PM machines are presented in Table I and Fig. 8.

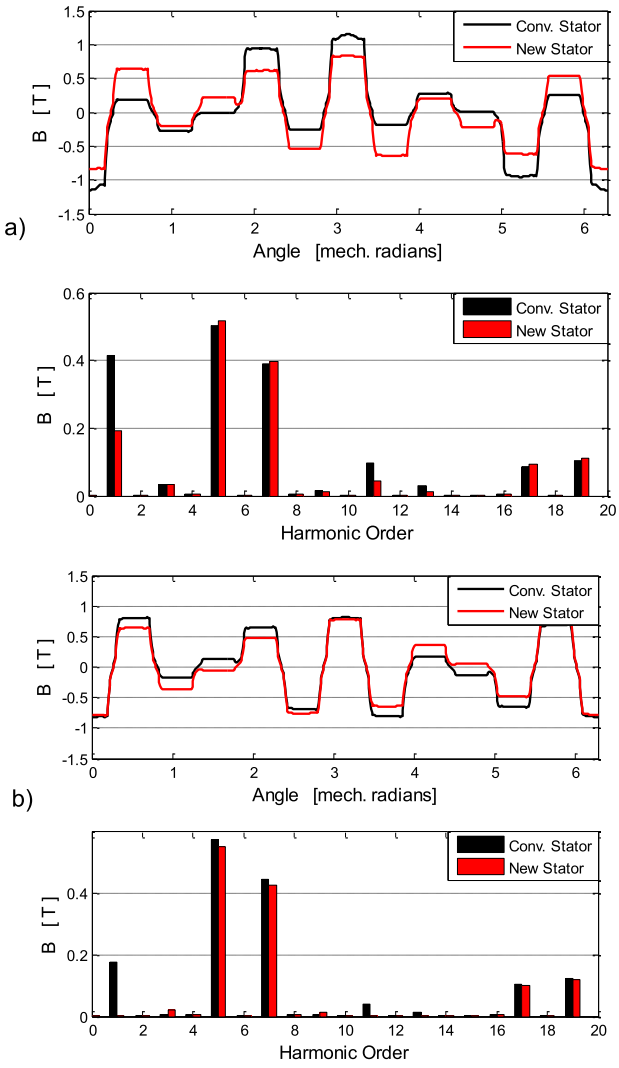

Fig. 10. Air-gap flux density due to armature reaction field. (a) Single-layer winding. (b) Double-layer winding.

The flux barrier depth for the single- and double-layer design is taken to be $0.95 \cdot h_Y$ and $0.65 \cdot h_Y$, respectively. For all machine designs, the electrical and geometrical constrains are taken to be the same ($U_{\mathrm{DC}} = 12$ V, $I_{\max} = 70$ Arms, and volume: $D_{\mathrm{Out}} = 81$ mm and $L_{\mathrm{Stack}} = 70$ mm). Furthermore, the same rotor design is considered for the all examples; the only difference on the investigated machine geometries is the stator core (with and without flux barriers) and the winding layout (single/double layer).

The simulation results presented in the following are performed using FEM. The considered electric machines are investigated under the same load condition (50 Arms load current).

A. Air-Gap Flux Density

For the armature reaction field under $I = 50$ Arms and $\delta = 20°$ three-phase load condition, the flux line distribution is shown in Fig. 9, and the behavior of the flux density in the middle of air gap is shown in Fig. 10. It can be observed here that, using a proper new stator design, the

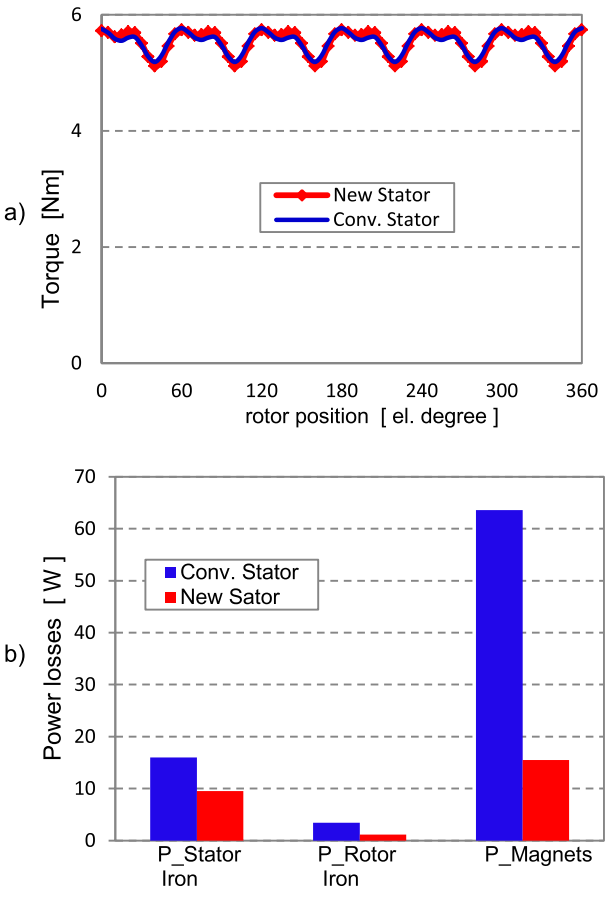

Fig. 11. Single-layer machine design. (a) Electromagnetic torque for $I_{\text{eff}} = 5\text{aA}$. (b) Power losses for $I_{\text{eff}} = 5\text{aA}$ and $n = 1000$ rpm.

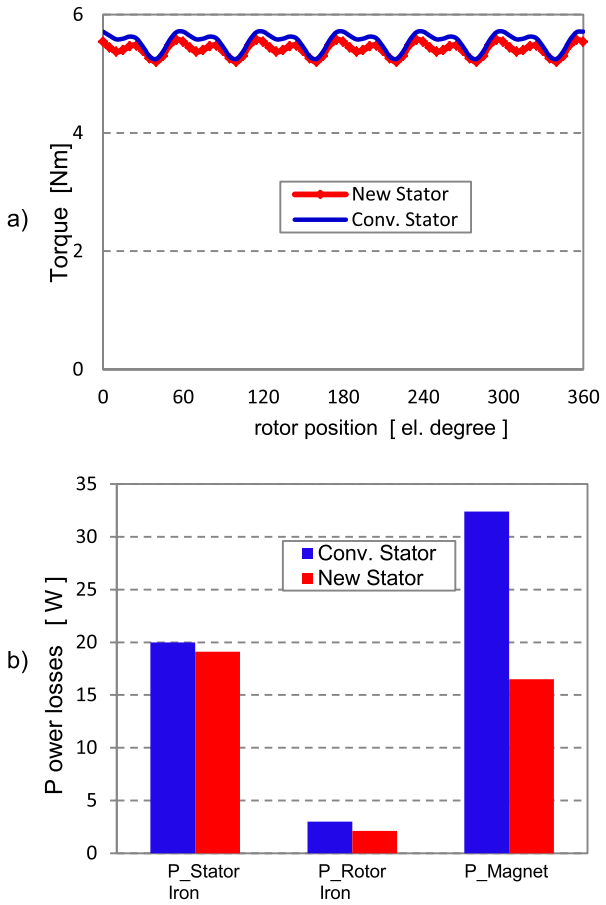

Fig. 12. Double-layer machine design. (a) Electromagnetic torque for $I_{\text{eff}} = 5\text{aA}$. (b) Power losses for $I_{\text{eff}} = 5\text{aA}$ and $n = 1000$ rpm.

air-gap flux density subharmonics can be reduced more than 60% for the single-layer winding; however, for the double-layer winding, the subharmonics completely are canceled. On other side, the working harmonic for the single-layer winding is slightly improved; however, in contrast, for the double-layer winding as results of flux barriers, it is reduced for about 3%.

B. Electromagnetic Torque and Power Losses

For the same load condition as above, the effect of the flux barriers on the electromagnetic torque and power losses is shown in Figs. 11 and 12. For the double-layer winding, the average torque is reduced for about 3%, while for the single-layer winding, it remains the same. It is important to point out that the torque reduction for the double-layer winding is mainly as results of the flux barrier effect on the air-gap flux density working (fifth) harmonic.

Furthermore, comparing the machine losses under the given excitation current and at 1000 r/m, for the both winding topologies, they are reduced enormously with the new stator design. A loss reduction up to 40% for the stator iron, 60% for the rotor iron, and up to 80% for the magnets is achieved. Therefore, the new stator design shows significant improvements on the efficiency of the electric machines with concentrated windings.

C. Machine Parameters

The machine parameters play a key role in determining various aspects of the PM machine characteristics, such as the flux-weakening (FW) capability, torque components, fault currents, and so on. The analysis of a PM machine is conveniently carried out in a d–q rotating reference frame. The steady-state equations for the voltage and the electromagnetic torque are

$$u_d = R \cdot i_d - \omega L_q \cdot i_q - \omega \psi_q^m$$
$$u_q = R \cdot i_q + \omega L_d \cdot i_d + \omega \psi_d^m \quad (9)$$
$$T_e = \frac{3}{2} p \left[(L_d - L_q) \cdot i_d \cdot i_q + \left(\psi_d^m \cdot i_q - \psi_q^m \cdot i_d \right) \right] \quad (10)$$

where ψ^m is the flux linkage due to the PMs, L is the machine inductance, and T_e is the electromagnetic torque. Furthermore, the dq-indexes represent the d- and q-axis components of the machine parameters.

To examine the influence of the magnetic flux barriers on the machine parameters, the finite-element (FE) investigations performed in following are carried out for 50 Arms load current and different current angles. To consider the saturation effect on the machine parameters and also the cross-coupling effect in the two-axis model, the fixed permeability method is implemented in the FE model during the determination of the dq-parameters [27], [28]. The variations of the dq-machine parameters for different load conditions are shown

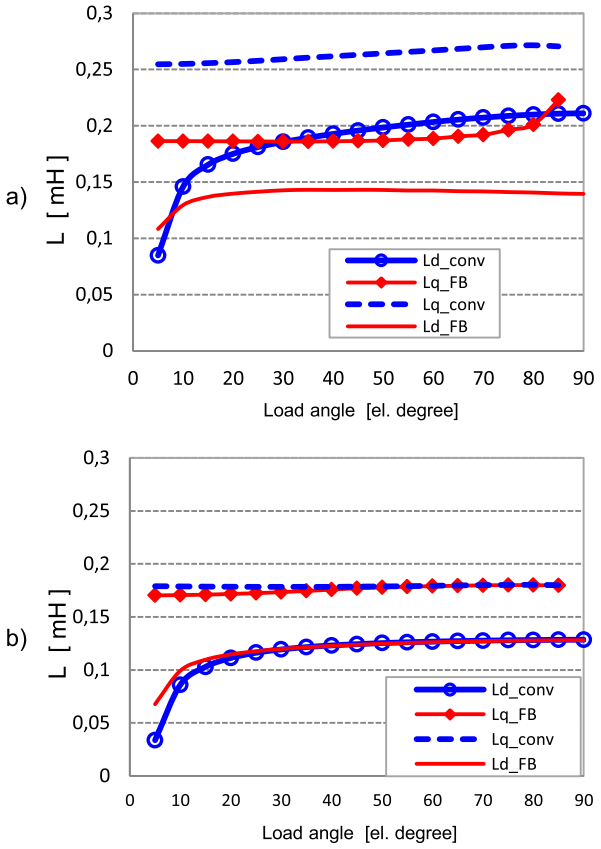

Fig. 13. dq-inductances versus current load angle for $I_{\text{eff}} = 50$ A. (a) Single-layer winding. (b) Double-layer winding.

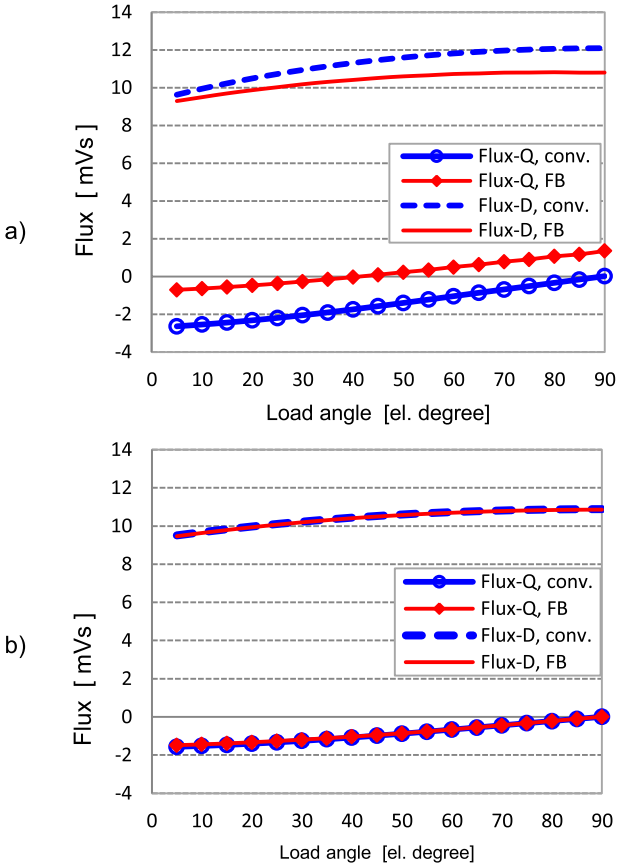

Fig. 14. dq PM flux linkage versus current load angle for $I_{\text{eff}} = 50$ A. (a) Single-layer winding. (b) Double-layer winding.

in Figs. 13 and 14. As expected, for the conventional stator design, the dq-inductances for the single-layer winding are higher compared with double-layer winding. Depends on the load operation condition, the ratio between these inductances is between 1.5 and 1.6, which is in good agreement with the results presented in [23]. However, comparing the results for the conventional and the new stator design, it can be observed that, for the single-layer winding, the flux barriers have a considerable effect on the dq-inductance results. Otherwise, for the double-layer winding, its effect is negligible. To have a clear explanation about the flux barrier effects on the machine inductances in Fig. 15, we have presented the flux lines distribution due to stator currents under one-phase excitation condition. As well is shown here, for the single-layer machine design, the flux barriers reduce completely the coupling effect between the phase coils (opposite coils of one phase). The flux lines for this case are analogously distributed as for the double-layer winding design with the conventional stator. Therefore, the reduction of the coupling effect and also of the first subharmonic leads to the reduction of dq-inductance parameters. On the other side, for the double-layer winding design, the flux barrier effect on the dq-inductances is minimal, even in the flux density, we can observe a more uniform distribution of the flux lines around the air gap than for the conventional stator. In contrast to the single-layer winding, the relative amount of the first subharmonic in the winding inductances is clearly small, and therefore the reduction of this harmonic has a negligible effect on the machine inductances. Furthermore, analogous to the machine inductances, the flux barrier effect on the PM flux-linkage components is present only for the single-layer winding.

D. Field-Weakening Characteristics

Nowadays, the electric machines are mostly fed from pulsewidth-modulated frequency inverters and are designed for application in variable speed drives. One of the main requirements for different industry applications, such as in automotive, is the wide operation speed range (OSR) capability. In general, the maximum speed of a PM machines is limited by the inverter current and voltage ratings. Wide OSR can be achieved either by employing an inverter with higher voltage rating or by reducing the back EMF of the machine using field weakening (FW) techniques. The field-weakening capability of PM machines depends on the machine parameters and particularly from the winding inductances. In general, PM machines with concentrated windings are characterized with high winding inductance and thus with high FW capability [24]–[26]. According to [24], the characteristic current I_{ch} is the best indicator for the FW capability of PM machines, which is defined as follows:

$$I_{\text{ch}} = \psi_d^m / L_d \quad \text{(Arms)}. \tag{11}$$

It has been shown in [24] that the condition for optimal FW in an PM machine can be achieved using concentrated

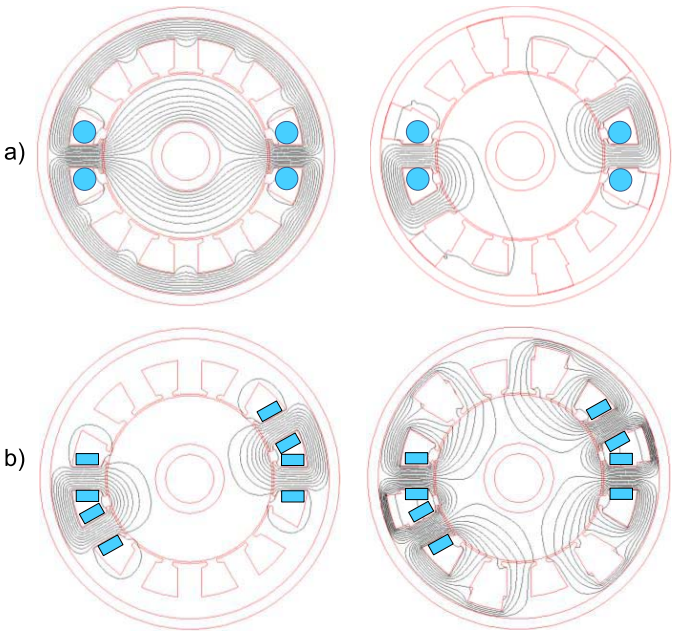

Fig. 15. Flux line distribution due to the armature reaction field under one-phase excitation condition ($Ia = 50$ arms and $Ib = Ic = 0$ arms). (a) Single-layer winding. (b) Double-layer winding.

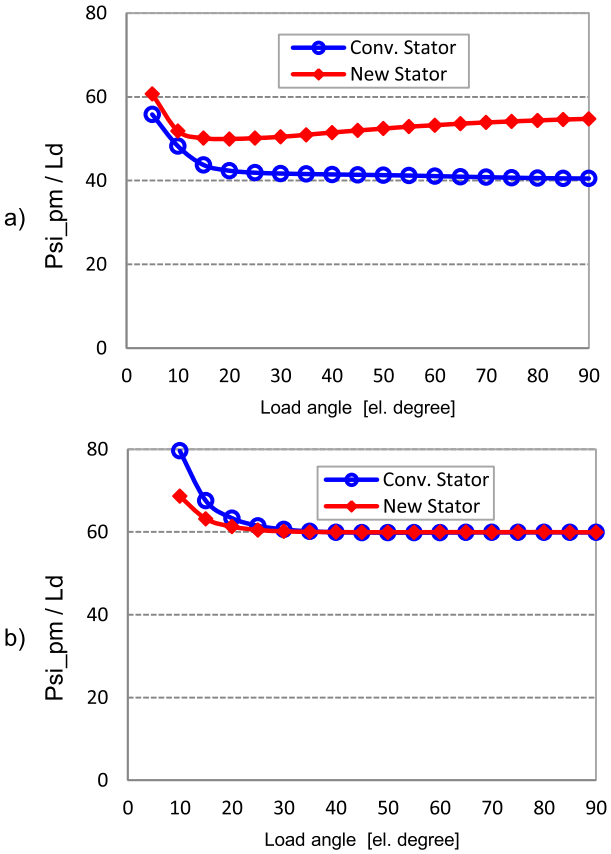

Fig. 16. Characteristic current versus current load angle for $I_{\text{eff}} = 50$ A. (a) Single-layer winding. (b) Double-layer winding.

windings with high winding inductances to limit the characteristic current. Fig. 16 shows the characteristic currents for the considered machines with and without flux barriers in stator. The values for the machine parameters given in previous

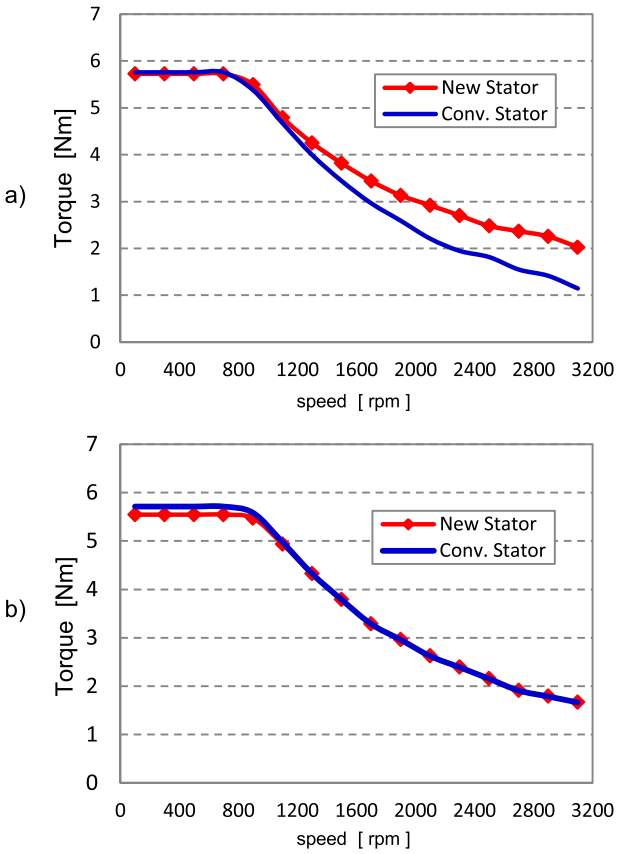

Fig. 17. Electromagnetic torque versus rotor speed for $I_{\text{eff}} = 50$ A. (a) Single-layer winding. (b) Double-layer winding.

section are used in (11) for the determination of I_{ch}. It can be observed from Fig. 16 that, for the single-layer winding type, the flux barriers increase the characteristic current up to 32%; however, for the double-layer winding, its effect is negligible. Therefore, at the first point of view, regarding to the field-weakening capability, the new stator design shows to be not a good solution for the single-layer PM machines. However, the torque–speed characteristics that are obtained according to the previous relations (9) and (10) and under the fixed 12 V dc voltage condition show the contrary. The obtained results shown in Fig. 17(a) show that the flux barriers improve significantly the torque–speed characteristics for the single-layer design. Therefore, considering these results, it can be concluded that only a high d-axis inductances is not responsible for a good field-weakening capability; however, according to voltage equations given in (9), both L_d and L_q inductance parameters are responsible for the maximal voltage and field-weakening characteristics of the machine. The resulting voltage components in function of speed are shown in Fig. 18. As results of the high L_q inductance for the conventional stator design, the u_d voltage increases rapidly with the rotor speed, and the sum of voltage components $(u_q^2 + u_d^2)$ reaches early the voltage limit and also the field-weakening region. On the other side, for the considered load current, the high L_d inductance leads to an over weakening of the magnet flux that results to a linear increase of the u_q voltage with the speed in the negative region. Therefore, the reduction of the dq-inductance for the single-layer winding using flux barriers

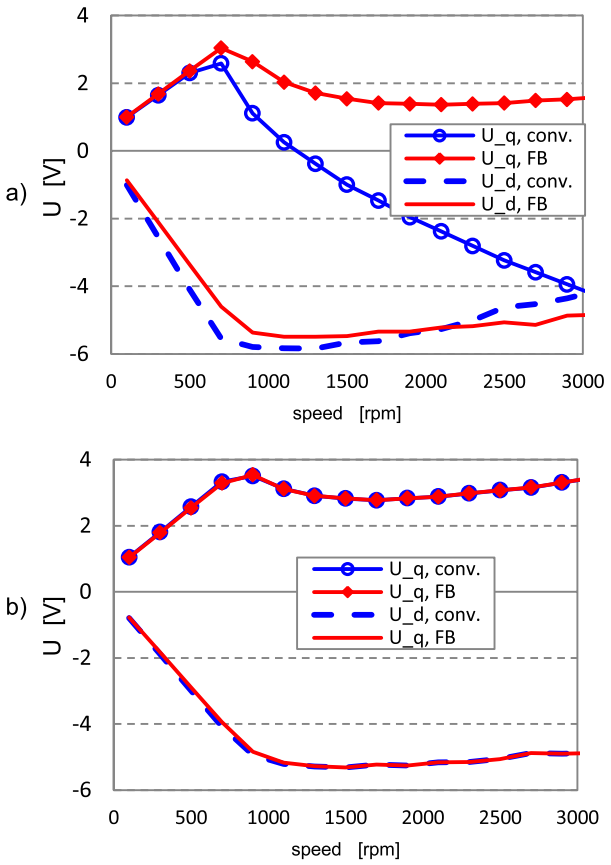

Fig. 18. *dq*-voltage components versus rotor speed for $I_{\text{eff}} = 50$ A. (a) Single-layer winding. (b) Double-layer winding.

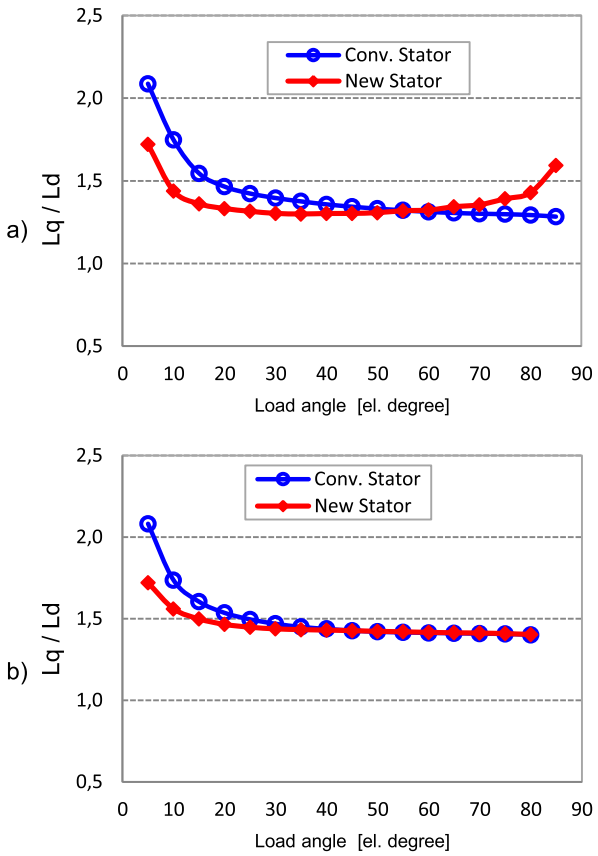

Fig. 19. Flux barrier effect on the reluctance components for $I_{\text{eff}} = 50$ A. (a) Single-layer winding. (b) Double-layer winding.

improves the field-weakening characteristics for this winding type. In addition, as shown in Fig. 19, the flux barriers do not degrade the reluctance torque component of the machine.

V. Prototype Machine

According to the new PM machine design with the 12-teeth/10-poles double-layer winding, a prototype machine is built and tested. Fig. 20 shows the geometry for the prototype machine. The stator core consists of 12 simple tooth/yoke stator segments of iron core material and of six additional stator yoke components of nonmagnetic material, which are used as flux barriers and also for fixing (mounting) the complete stator structure. The rotor consists of a simple core structure with 10 rectangular magnets. Fig. 21 shows the stator structure for the prototype machine during manufacturing. For fixing the stator components, two end rings are used on both stator sides, and using a proper combinations of the flux barriers and the end ring components, the prototype machine is built as frameless machine. Therefore, according to the simple machines structure and design in following, this machine type is called as low-cost (LC) motor.

It is important to point out that, in the presented prototype machine, the flux barriers in the stator yoke are built by dividing completely the yoke region, and according to Fig. 7, using a ratio of 100% for the double layer has no effect in the fundamental harmonic. However, in the prototype design, the same effect as in Fig. 7 (for 65% flux barrier depth ratio)

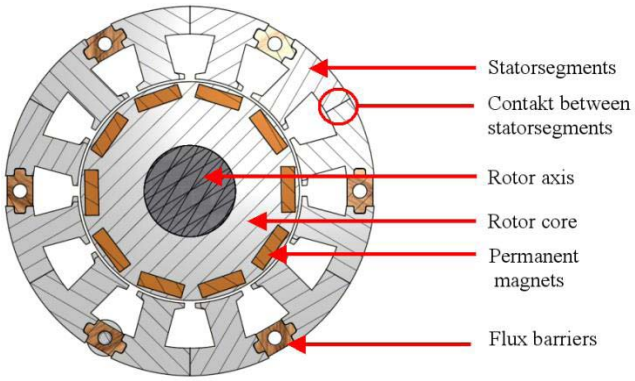

Fig. 20. Geometry of the designed LC PM machine.

is achieved using an optimally shape geometry for the flux barrier regions and also an optimal relation between *hw* and *hy* flux barrier geometry parameters.

VI. Experimental Result

Fig. 22 and Table II show the test bench for the LC motor and the main machine parameters. The maximum torque per ampere (MTPA) control method [29], [30] is used during the measurements of the LC motor characteristics for the steady-state and transient analysis. The key point of MTPA is to achieve MTPA by providing a combination of d-axis current i_d

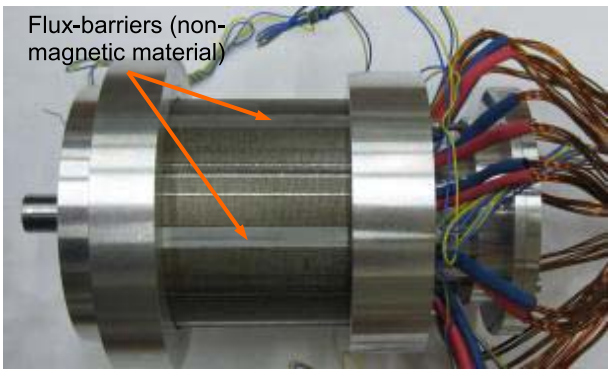

Fig. 21. Designed LC PM machine prototype.

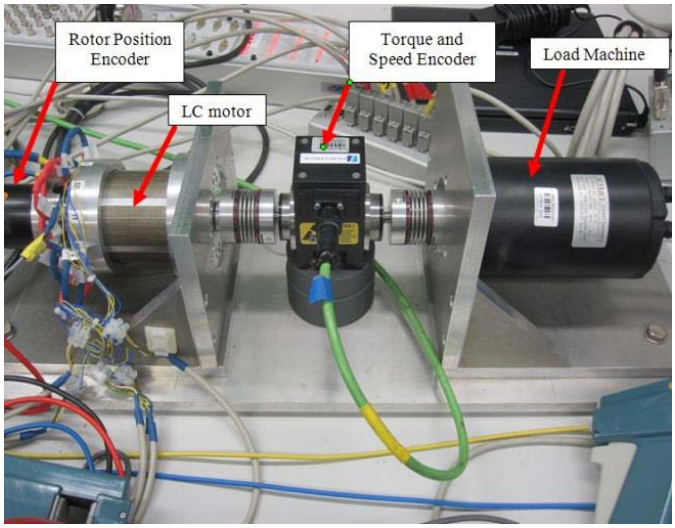

Fig. 22. Practical LC motor measurement setup.

TABLE II
MAIN LC MOTOR PARAMETERS

Number of pole pairs	p	5
Stator resistance	R_s	$18m\Omega$
d axis inductance	L_d	$0.05mH$
q axis inductance	L_q	$0.095mH$
Permanent magnet flux	ψ^m	$7.07mVs$
DC link voltage	U_{dc}	12V
Rated torque	T_N	2Nm

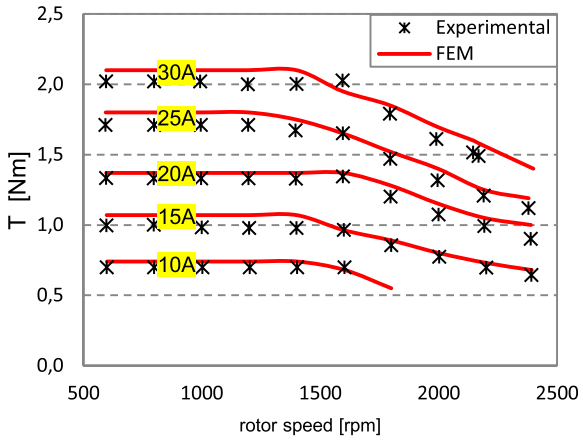

Fig. 23. Torque versus speed characteristics of LC motor.

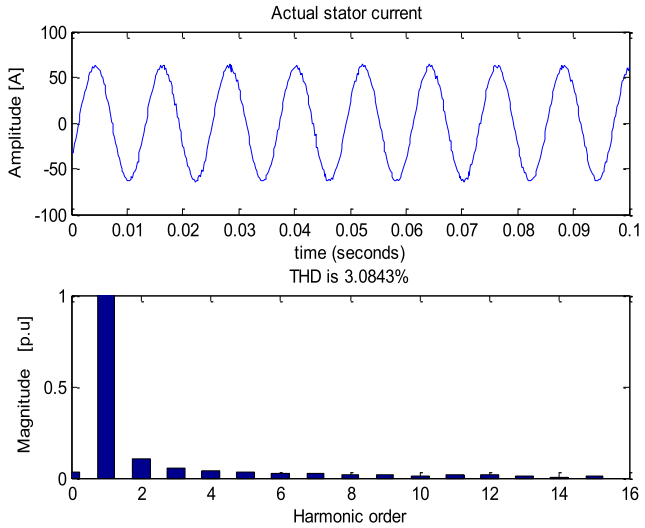

Fig. 24. Current quality for 2 Nm and 1000 r/m operation point.

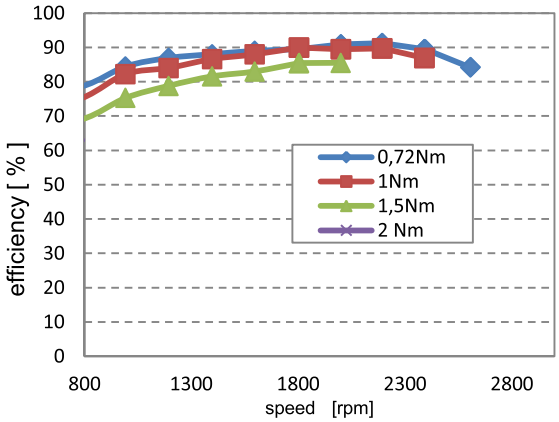

Fig. 25. Experimental results and machine efficiency.

and q-axis current i_q. For surface mounted PM (SMPM) machines, due to $L_d = L_q$, the electromagnetic torque T_e and i_q have a linear relationship whether i_d is equal to zero or not. Thus, based on $i_d = 0$, the vector control of SMPM machines can achieve the MPTA effect. Different with SMPM, because of saliency effect ($L_d \neq L_q$) of considered prototype machine (interior PM in rotor), i_d of MTPA for IPMSM is not equal to zero, and for the rotor speed below the base speed, the reference i_d is determined from (12). However, with the speed increasing, since the machine voltage is limited by dc-link voltage of inverter, the FW method is used to increase the torque under high speed the reference i_d will change to (13) [31]. The switching speed of these two control strategies

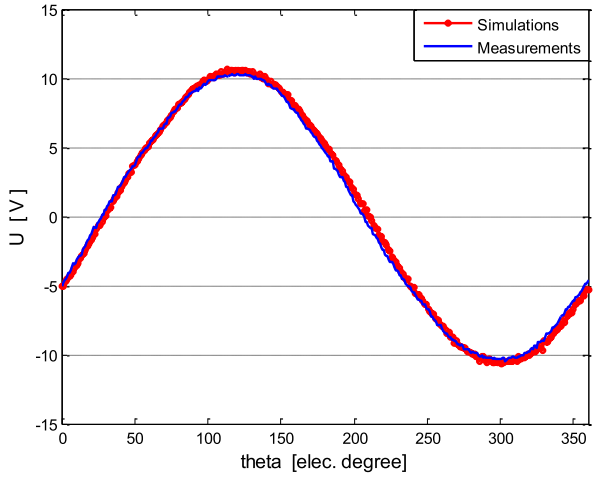

Fig. 26. No-load induced voltage at 3000 r/m.

is 1580 r/m

$$i_d^* = \frac{\psi^m - \sqrt{(\psi^m)^2 + 8\left(L_q - L_d\right)^2 i_q^2}}{4\left(L_q - L_d\right)} \tag{12}$$

$$i_d^* = -\frac{\psi^m}{L_q} + \sqrt{\left(\frac{U_{dc}}{\sqrt{2}L_d \cdot \omega_e}\right)^2 - \left(\frac{L_q \cdot i_q}{L_d}\right)^2}. \tag{13}$$

The drive performances of LC motor are shown in Figs. 23–26. Fig. 23 shows the torque–speed characteristic for different stator load currents, the current quality for 2 Nm and at 1000 r/m is shown in Fig. 24, and the machine efficiency is shown in Fig. 25. Furthermore, the FE predicted and the measured per phase voltage of the prototype PM machine are shown in Fig. 26. The comparison of results show a good agreement between the experimental and FEM data.

VII. Conclusion

A novel method for reducing of the air-gap flux density subharmonics for the fractional slot tooth-concentrated windings using magnetic flux barriers in stator yoke is presented. Using the new stator structure, two 12-teeth/10-poles PM machines with different concentrated windings are investigated and their performances are compared with the conventional stator design. Considering the main machine parameters, such as the electromagnetic torque, losses, and also the field-weakening capability, the obtained results show that the new stator design brings significant advantages over the conventional design, such as:

1) subharmonic reduction more than 60%;
2) power loss reduction up to 40% for the stator iron losses, 60% for the rotor iron losses, and up to 80% for the magnet losses;
3) high field-weakening capability.

The design and analysis of the considered machines presented in this paper is performed using FEM. For the PM machine design with the double-layer winding, a prototype machine with the new stator structure is built and different measurement results for the toque–speed characteristics, phase current, machine efficiency, and no-load induced voltage are given. The experimental results on prototype machine demonstrate the applicability of the new technique.

References

[1] F. Libert and J. Soulard, "Investigation on pole-slot combinations for permanent-magnet machines with concentrated windings," in *Proc. ICEM*, Cracow, Poland, Sep. 2004, pp. 1–5.
[2] J. Wang, K. Atallah, Z. Q. Zhu, and D. Howe, "Modular three-phase permanent-magnet brushless machines for in-wheel applications," *IEEE Trans. Veh. Technol.*, vol. 57, no. 5, pp. 2714–2720, Sep. 2008.
[3] F. Magnussen and C. Sadarangani, "Winding factors and Joule losses of permanent magnet machines with concentrated windings," in *Proc. IEEE IEMDC*, vol. 1. Madison, WI, USA, Jun. 2003, pp. 333–339.
[4] J. Li, D. W. Choi, D. H. Son, and Y. H. Cho, "Effects of MMF harmonics on rotor eddy-current losses for inner-rotor fractional slot axial flux permanent magnet synchronous machines," *IEEE Trans. Magn.*, vol. 48, no. 2, pp. 839–842, Feb. 2012.
[5] K. Yamazaki and Y. Fukushima, "Effect of eddy-current loss reduction by magnet segmentation in synchronous motors with concentrated windings," *IEEE Trans. Ind. Appl.*, vol. 47, no. 2, pp. 779–788, Mar./Apr. 2011.
[6] N. Bianchi and E. Fornasiero, "Index of rotor losses in three-phase fractional slot permanent magnet machines," *IET Electr. Power Appl.*, vol. 3, no. 5, pp. 381–388, Sep. 2009.
[7] J. Wang, K. Atallah, R. Chin, W. M. Arshad, and H. Lendenmann, "Rotor eddy-current loss in permanent-magnet brushless AC machines," *IEEE Trans. Magn.*, vol. 46, no. 7, pp. 2701–2707, Jul. 2010.
[8] A. M. EL-Refaie, M. R. Shah, R. Qu, and J. M. Kern, "Effect of number of phases on losses in conducting sleeves of surface PM machine rotors equipped with fractional-slot concentrated windings," *IEEE Trans. Ind. Appl.*, vol. 44, no. 5, pp. 1522–1532, Sep./Oct. 2010.
[9] H. Polinder, M. J. Hoeijmakers, and M. Scuotto, "Eddy-current losses in the solid back-iron of PM machines for different concentrated fractional pitch windings," in *Proc. IEMDC*, Antalya, Turkey, May 2007, pp. 652–657.
[10] G. Dajaku and D. Gerling, "Magnetic radial force density of the PM machine with 12-teeth/10-poles winding topology," in *Proc. IEMDC*, Miami, FL, USA, May 2009. pp. 157–164.
[11] J. Wang, Z. P. Xia, D. Howe, and S. A. Long, "Vibration characteristics of modular permanent magnet brushless AC machines," in *Proc. IEEE 41st IAS Annu. Meeting Ind. Appl. Conf.*, Tampa, FL, USA, Oct. 2006, pp. 1501–1506.
[12] G. Dajaku and D. Gerling, "The influence of permeance effect on the magnetic radial forces of permanent magnet synchronous machines," *IEEE Trans. Magn.*, vol. 49, no. 6, pp. 2953–2966, Jun. 2013.
[13] J. Krotsch and B. Piepenbreier, "Radial forces in external rotor permanent magnet synchronous motors with non-overlapping windings," *IEEE Trans. Ind. Electron.*, vol. 59, no. 5, pp. 2267–2276, May 2012.
[14] M. V. Cistelecan and F. J. T. E. Ferreira, "Three phase tooth-concentrated multiple-layer fractional windings with low space harmonic content," in *Proc. IEEE ECCE*, Sep. 2010, pp. 1399–1405.
[15] E. Farnasiero, L. Alberti, N. Bianchi, and S. Bolognani, "Considerations on selecting fractional–Slot windings," in *Proc. IEEE ECCE*, Sep. 2010, pp. 1376–1383.
[16] K. Ito, K. Naka, M. Nakano, and M. Kobayashi, "Electric machine," U.S. Patent 7 605 514, Oct. 20, 2009.
[17] M. Cistelecan, F. F. Ferreira, and M. Popescu, "Three-phase tooth-concentrated interspersed windings with low space harmonic content," in *Proc. 19th ICEM*, Rome, Italy, Sep. 2010, pp. 1–6.
[18] G. Dajaku and D. Gerling, "Eddy current loss minimization in rotor magnets of PM machines using high-efficiency 12-teeth/10-poles winding topology," in *Proc. ICEMS*, Beijing, China, Aug. 2011, pp. 1–6.
[19] G. Dajaku and D. Gerling, "A novel 12-teeth/10-poles PM machine with flux barriers in stator yoke," in *Proc. 20th ICEM*, Marseille, France, Sep. 2012, pp. 36–40.
[20] G. Dajaku and D. Gerling, "Low costs and high-efficiency electric machines," in *Proc. 2nd Int. EDPC*, Nuremberg, Germany, Oct. 2012, pp. 1–7.
[21] G. Dajaku and D. Gerling, "A novel 24-slots/10-poles winding topology for electric machines," in *Proc. IEEE IEMDC*, Niagara Falls, ON, Canada, May 2011, pp. 65–70.
[22] G. Dajaku and D. Gerling, "A novel tooth concentrated winding with low space harmonic content," in *Proc. IEEE IEMDC*, Chicago, IL, USA, May 2013, pp. 755–760.

[23] D. Ishak, Z. Q. Zhu, and D. Howe, "Comparison of PM brushless motors, having either all teeth or alternate teeth wound," *IEEE Trans. Energy Convers.*, vol. 21, no. 1, pp. 95–103, Mar. 2006.
[24] R. Dutta, L. Chong, and M. F. Rahman, "Winding inductances of an interior permanent magnet (IPM) machine with fractional slot concentrated winding," *IEEE Trans. Magn.*, vol. 48, no. 12, pp. 4842–4849, Dec. 2012.
[25] J. Cros, J. R. Figueroa, and P. Viarouge, "BLDC motors with surface mounted PM rotor for wide constant power operation," in *Proc. 38th IAS Annu. Meeting, Conf. Rec. Ind. Appl. Conf.*, vol. 3. Oct. 2003, pp. 1933–1940.
[26] A. M. EL-Refaie and T. M. Jahns, "Scalability of surface PM machines with concentrated windings designed to achieve wide speed ranges of constant-power operation," *IEEE Trans. Energy Convers.*, vol. 21, no. 2, pp. 362–369, Jun. 2006.
[27] Z. Jibin and L. Weiyan, "Analytical modelling finite element calculation of the saturation DQ-axes inductance for a direct drive PM synchronous motor considering cross-magnetization," in *Proc. 5th Int. Conf. PEDS*, Nov. 2003, pp. 677–681.
[28] N. Bianchi and S. Bolognani, "Magnetic models of saturated interior permanent magnet motors based on finite element analysis," in *Proc. IEEE 33rd IAS Annu. Meeting, Ind. Appl. Conf.*, vol. 1. Oct. 1998, pp. 27–34.
[29] P. Niazi, H. A. Toliyat, and A. Goodarzi, "Robust maximum torque per ampere (MTPA) control of PM-assisted SynRM for traction application," *IEEE Trans. Veh. Technol.*, vol. 56, no. 4, pp. 1538–1545, Jul. 2007.
[30] S. Kim, Y. D. Yoo, S. K. Sul, and K. Ide, "Maximum torque per ampere (MTPA) control of an IPM machine based on signal injection considering inductance saturation," *IEEE Trans. Power Electron.*, vol. 28, no. 1, pp. 488–497, Jan. 2013.
[31] V. C. Ilioudis and N. I. Margaris, "Flux weakening method for sensorless PMSM control using torque decoupling technique," in *Proc. 1st Symp. SLED*, Jul. 2010, pp. 32–39.

Gurakuq Dajaku was born in Skenderaj, Kosova, in 1974. He received the Diploma degree in electrical engineering from the University of Prishtina, Prishtina, Kosova, and the Ph.D. degree from Universitaet der Bundeswehr Muenchen, Munich, Germany, in 1997 and 2006, respectively.

He has been a Senior Scientist with FEAAM GmbH, since 2007, which is an engineering company in the field of electric drives. Since 2008, he has been a Lecturer with Universitaet der Bundeswehr Muenchen. He has published numerous technical papers in different IEEE journals and conferences and has several international patents and patent pending applications. His current research interests include electrical machines and drives.

Dr. Dajaku received the Rheinmetall Foundation Award in 2006 and the Institute for Technical Intelligent Systems Research Award in 2006.

Wei Xie (S'13) was born in China in 1982. He received the master's degree in electrical engineering from Northwestern Polytechnical University, Xi'an, China, in 2011. He is currently pursuing the Ph.D. degree with the University of Federal Defense Munich, Munich, Germany.

His current research interests include self-sensing control for synchronous machines.

Dieter Gerling was born in Menden, Germany, in 1961. He received the Diploma and Ph.D. degrees in electrical engineering from the Technical University of Aachen, Aachen, Germany, in 1986 and 1992, respectively.

He was with the Philips Research Laboratories, Aachen, as a Research Scientist, from 1986 to 1999, and later as a Senior Scientist. In 1999, he was with Robert Bosch GmbH, Bühl, Germany, as a Director. Since 2001, he has been a Full Professor with Universitaet der Bundeswehr Muenchen, Munich, Germany.